THE JOURNAL OF BIOLOGICAL CHEMISTRY VOL. 286, NO. 50, pp. 43103–43111, December 16, 2011

Close-up of the Immunogenic α1,3-Galactose Epitope as Defined by a Monoclonal Chimeric Immunoglobulin E and Human Serum Using Saturation Transfer Difference (STD) NMR[S]

Received for publication, August 23, 2011, and in revised form, October 3, 2011 Published, JBC Papers in Press, October 11, 2011, DOI 10.1074/jbc.M111.291823

Melanie Plum[‡1], **Yvonne Michel**[‡1], **Katharina Wallach**[§1], **Tim Raiber**[‡], **Simon Blank**[‡], **Frank I. Bantleon**[‡], **Andrea Diethers**[‡], **Kerstin Greunke**[‡], **Ingke Braren**[¶], **Thomas Hackl**[§], **Bernd Meyer**[§], **and Edzard Spillner**[‡2]

From the [‡]*Institute of Biochemistry and Molecular Biology and the* [§]*Institute of Organic Chemistry, University of Hamburg, Hamburg 20146 , Germany and the* [¶]*Hamburg Center for Experimental Therapy Research, University Medical Center Hamburg-Eppendorf, Hamburg 20246, Germany*

Background: Antibody binding to xenobiotic α-Gal structures mediates anaphylaxis.
Results: Humanized IgE antibodies exhibit recognition footprints similar to serum immunoglobulins but have no capability of effector cell activation.
Conclusion: Recognition of the α-Gal epitope is based on the terminal disaccharide, but interaction does not imply cellular activation.
Significance: These data provide the first insights into the recognition of carbohydrate IgE epitopes.

Anaphylaxis mediated by carbohydrate structures is a controversially discussed phenomenon. Nevertheless, IgE with specificity for the xenotransplantation antigen α1,3-Gal (α-Gal) are associated with a delayed type of anaphylaxis, providing evidence for the clinical relevance of carbohydrate epitopes in allergy. The aim of this study was to dissect immunoreactivity, interaction, and fine epitope of α-Gal-specific antibodies to obtain insights into the recognition of carbohydrate epitopes by IgE antibodies and their consequences on a molecular and cellular level. The antigen binding moiety of an α-Gal-specific murine IgM antibody was employed to construct chimeric IgE and IgG antibodies. Reactivity and specificity of the resulting antibodies were assessed by means of ELISA and receptor binding studies. Using defined carbohydrates, interaction of the IgE and human serum was assessed by mediator release assays, surface plasmon resonance (SPR), and saturation transfer difference NMR analyses. The α-Gal-specific chimeric IgE and IgG antibodies were proven functional regarding interaction with antigen and Fc receptors. SPR measurements demonstrated affinities in the micromolar range. In contrast to a reference antibody, anti-Gal IgE did not induce mediator release, potentially reflecting the delayed type of anaphylaxis. The α1,3-Gal epitope fine structures of both the recombinant IgE and affinity-purified serum were defined by saturation transfer difference NMR, revealing similar contributions of carbohydrate residues and participation of both galactose residues in interaction. The antibodies generated here constitute the principle underlying α1,3-Gal-mediated anaphylaxis. The complementary data of affinity and fine specificity may help to elucidate the recognition of carbohydrates by the adaptive immune response and the molecular requirements of carbohydrate-based anaphylaxis.

Circulating concentrations of IgE, the antibody class responsible for allergic hypersensitivity, are linked to the development of several immunity-mediated diseases (1). IgE antibodies bound to their high affinity receptor (FcεRI) on mast cells and basophils mediate receptor cross-linking by allergens and trigger degranulation and release of proinflammatory mediators responsible for immediate-type hypersensitivity reactions. However, the exact interplay of different isotypes with their cognate allergens remains enigmatic.

Apart from the protein backbone, IgG and IgE may also be directed against xenobiotic and therefore immunogenic and cross-reactive carbohydrate determinants (CCDs)[3] present on a plethora of proteins found in food, pollen, and hymenoptera venom (2). The hallmark of classical CCDs are α1,3-linked core fucose residues found on insect venom allergens, and, additionally, β1,2-linked xylose on plant-derived CCDs. Antibody specificity for these spatially separated glycotopes represents the universal principle for reactivity of different proteins having CCDs (3). The role of CCDs as a cause of allergic symptoms still is controversial (4). IgE against classical CCDs has been shown to be clinically relevant (5–8), but artificial or recombinant glycoproteins did not show clear cut effects in mediator release assays or skin prick tests (9, 10).

Recently, a novel type of CCD has entered the field and provided final evidence for the detrimental potential of glycans.

[S] The on-line version of this article (available at http://www.jbc.org) contains supplemental Figs. 1 and 2.
[1] Both authors contributed equally to this work.
[2] To whom correspondence should be addressed: Institute of Biochemistry and Molecular Biology, Dept. of Chemistry, University of Hamburg, Martin-Luther-King-Platz 6, 20146 Hamburg, Germany. Tel.: 49-40-42838-6982; Fax: 49-40-42838-7255; E-mail: spillner@chemie.uni-hamburg.de.

[3] The abbreviations used are: CCD, cross-reactive carbohydrate determinant; α-Gal, α1,3-Gal; STD, saturation transfer difference; scFv, single chain Fv; SPR, surface plasmon resonance; HSA, human serum albumin; MPBS, milk powder PBS.

Clearly IgE-mediated anaphylaxis via the well established Gal-α1,3-Gal structure (α-Gal) as present on the chimeric therapeutic antibody cetuximab could be shown (11). This epitope is also essential in meat-induced allergy (12) and for cross-reactivity to other mammalian allergens (13). Strong induction of α-Gal-specific IgE very recently was correlated with bites of tick species present within a restricted area of the United States (14).

Anti-Gal IgG antibodies, especially of the IgG2 subclass, constitute up to 3% of serum immunoglobulins in humans, are induced by commensal bacteria, and putatively exert a natural barrier function (15). Their clinical relevance is well documented for xenotransplantation and blood group antigens, providing α1,3-linked galactose residues, resulting in hyperacute xenograft rejection (16). Scarce information however is available for α-Gal-specific IgE.

The interaction of polyclonal IgE with allergens has broadly been studied, but detailed analyses of the particularities of IgE and its epitopes are hampered by two critical limitations, the low IgE levels in serum and the lack of specific human monoclonal antibodies. Murine monoclonals often used as substitute are neither compatible with human cellular assays nor recognize authentic IgE epitopes and thus can provide indirect evidence only.

This limitation would be obsolete if murine antibodies recognized B-cell epitopes identical to those of human antibodies, a scenario only true for small sized epitopes that obey identical immunological mechanisms in animals and humans. Such a situation is presented for IgE with specificity for CCDs, which are defined by their high immunogenicity in different species and their spatially extraordinarily well defined architecture.

Structural and molecular data on the interaction of antibodies with carbohydrates (17–21) still are scarce and, particularly for the α-Gal epitope, poorly available. Molecular analyses of biomolecules with ligands of limited size, such as carbohydrates, can be obtained using saturation transfer difference (STD) NMR (22). Thereby, saturation is transferred from a receptor protein to ligands and leads to specific attenuation of resonance signals of ligands that bind to the receptor. This attenuation is made visible by difference spectroscopy and allows identification and characterization of the ligands and their interaction.

Thus, the aim of our work was to gain access to α-Gal-specific human antibody isotypes, allowing insights into the molecular and functional basis of their interaction. IgE and IgG were generated and employed for cellular activation tests and characterization of the IgE epitope by STD NMR. This work contributes to elucidation of the complex antibody carbohydrate interaction and molecular aspects in CCD-based anaphylaxis.

EXPERIMENTAL PROCEDURES

Production of Recombinant Antibodies—For establishing chimeric mouse/human antibodies, the VH and VL sequences of the α-Gal-specific antibody M86 was used as template for gene synthesis (23). Variable regions were assembled in the form of a single chain Fv (scFv) and introduced into phagemid vectors, allowing prokaryotic production as both soluble fragment and scFv-displaying phage.

Homodimeric IgG1 and IgE and heterotetrameric IgE immunoglobulins were produced using recently established vector systems (24). The variable regions VH and VL were amplified using oligonucleotides containing restriction sites at the 5′ and 3′ termini of the VH (gatcatttaaatgtgtccagtgtgaggtgaaactggag and gatcgtcgaccccgagacagtgacagaagttcc) and VL (gatccctgcagggtgccagatgtgatgtggtgatgacac and gatcggcgcgcccacagtccgtttgatttcgag) by PCR, respectively, in such a way that a 4× His tag is generated at the C-terminal end of the heavy chain. Subsequently, the DNA was introduced into the different expression vectors.

Human embryonic kidney cells (HEK-293, ATCC number CRL-1573) were cultivated in Dulbecco's modified Eagle's medium (DMEM) supplemented with 100 ml/liter fetal calf serum, 10 kallikrein-inactivating unit/liter penicillin, and 100 mg/liter streptomycin. Tissue culture reagents were obtained from Life Technologies. HEK-293 cells were transfected by using 3 μg of the particular expression vector DNA complexed with polyethylene imine (Sigma-Aldrich). The secreted immunoglobulins were purified from the culture medium by affinity chromatography using Ni^{2+}-NTA-agarose (Qiagen) according to the manufacturer's recommendations.

Amplification and Cloning of FcεRI-IgY Fc and CD64-IgY Fc—The cloning and expression of the soluble IgE Fc receptor FcεRI-IgY Fc has been described elsewhere (25). The human CD64 extracellular domains were amplified without the original signal sequence using one PCR primer containing a Pfl23II site (gatccgtacgtgtgggcaagtggacaccacaaaggc) and another primer containing an SgsI site (gatcggcgcgccatgaaaccagacaggagttgg) and introduced into pcDNA3.1/zeo, providing a rat immunoglobulin leader sequence and avian Fc regions (26).

Assessment of Immunoreactivity in ELISA—For assessment of immunoreactivity in direct ELISA, the particular proteins (10 μg/ml) were applied to microtiter plates, incubated at 4 °C overnight, and blocked with 4% MPBS at room temperature for 1 h. The recombinant immunoglobulins (1 μg/ml diluted with 2% MPBS) were added to the wells and incubated for 1 h at room temperature. The ELISA was performed according to established protocols and detected with human Ig isotype-specific antibody conjugates and *para*-nitrophenyl phosphate as a substrate at 405 nm.

The immunoreactivity of immunoglobulins with their particular Fc receptors was demonstrated by sandwich ELISA. Therefore, bovine thyroglobulin (50 μg/ml) was applied to microtiter plates, incubated at 4 °C overnight, and blocked with 4% MPBS at room temperature for 1 h. Thereafter, anti-Gal antibodies (1 μg/ml diluted with 2% MPBS) were added to the wells, incubated at room temperature for 1 h, and subsequently incubated with FcεRI-IgY Fc or CD64-IgY Fc (1 μg/ml diluted with 2% MPBS) according to established protocols and detected with a chicken IgG-specific antibody conjugate and *para*-nitrophenyl phosphate as a substrate at 405 nm.

For immunoblot procedures, the particular recombinant antibodies were separated by SDS-PAGE. Visualization was then performed with human Ig isotype-specific antibodies conjugated to alkaline phosphatase and nitrotetrazolium blue chloride/5-bromo-4-chloro-3-indoyl phosphate (nitro blue tetrazolium/5-bromo-4-chloro-3-indolyl phosphate).

In Vitro Mediator Release Assay with Humanized Rat Basophilic Leukemia Cells (RBL-SX38)—In vitro degranulation was analyzed as described previously (27). Soluble α-Gal proteins were biotinylated using TFPA-PEG3-biotin (tetrafluorophenylazide-(triethyleneglycol)-biotin (Pierce) according to the recommendations of the manufacturer and incubated with streptavidin-coated Roti-MagBeads (Roth). After sensitization of RBL-SX38 cells with IgE and washing with incomplete Tyrode's buffer (10 mM HEPES, pH 7.4, 130 mM NaCl, 5 mM KCl, 1.4 mM $CaCl_2$, 1 mM $MgCl_2$), α-Gal-carrying proteins or α-Gal-coated beads were added to the wells and incubated for 60 min at 37 °C. As a reference, cross-linking was achieved by the addition of polyclonal anti-human IgE serum (1 μg/ml from goat; Bethyl). β-Hexosaminidase release of viable *versus* lysed cells was assessed with *p*-nitrophenyl *N*-acetyl-glucosaminide (Sigma-Aldrich) as a substrate.

Surface Plasmon Resonance Analysis—The interaction affinity of cetuximab, α-Gal-HSA, thyroglobulin, and immobilized IgE as well as the affinity of a TNP-specific mouse IgE (clone C38-2) and immobilized TNP-BSA have been determined by surface plasmon resonance (SPR) measurements using the SPR-2 affinity sensor from Sierra Sensors (Hamburg, Germany). The IgE was covalently coupled to a total of 2400 resonance units on a carboxymethylated sensor chip surface (SPR-2 affinity sensor) using standard NHS/EDC coupling procedure via primary amines and capping by ethanolamine. The uncoupled surface served as reference. Measurements were performed at 20 °C in buffer containing 10 mM monosodium phosphate, 40 mM disodium phosphate, and 100 mM NaCl, pH 7.5, with 0.01% Tween 20. For the kinetic analyses, increasing concentrations of the α-Gal carrying antigens (7–167 nM for cetuximab, 121–564 nM for α-Gal-HSA, 15–120 nM for thyroglobulin) were injected at a flow rate of 25 μl/min. The association phase was monitored for 120 s, and the dissociation phase was monitored for 90 s. Sensor surfaces were regenerated after each binding cycle by two subsequent injections of 50 mM Tris buffer, pH 10. After subtracting reference cell signals, the resulting binding data were fitted to a Langmuir 1:1 binding model by using global fit analysis (evaluation software, Sierra Sensors), and the dissociation constant at equilibrium, K_D, was calculated.

STD NMR—Buffer exchange against deuterated PBS and concentration of affinity-purified, anti-Gal-specific antibodies to 450 μg/ml were performed by using AMICON Ultra-4 10K centrifugal filter devices. Oligosaccharides were obtained from Dextra (Reading). The Gal-Gal disaccharide was purchased as methylglycoside and as biotinylated carbohydrate.

STD NMR experiments were performed at 298 K on a Bruker 500-MHz spectrometer equipped with a 5-mm inverse triple resonance probe head and a Bruker 700-MHz spectrometer equipped with a 5-mm inverse triple resonance probe head with cryotechnology. The PBS NMR buffer contained 137 mM NaCl, 2.7 mM KCl, 10 mM Na_2HPO_4, and 176 mM KH_2PO_4 in D_2O and was adjusted to pH 7.4. The on resonance pulse for antibody saturation was set to 0 Hz (500 MHz) or −500 Hz (700 MHz), respectively, and the off resonance pulse was set to 28,500 Hz (500 MHz) or 28,000 Hz (700 MHz). Saturation was achieved by a train of 90° Gaussian-shaped pulses of 50 ms, yielding a total saturation time of 2 s with an attenuation of 45 dB (500 MHz) or 40 dB (700 MHz). The spectra were acquired with a spectral width of 8000 Hz, 64000 time domain data points, and two transients using a pseudo-two-dimensional Bruker standard pulse sequence (*stddiff.3*, 500 MHz). A relaxation delay of 4 s was applied. For suppression of protein background, a $T_{1\rho}$ filter was used, applying a field strength of 11.5 kHz and a duration of 15 ms. Each experiment was performed with a total of 1024 scans. STD experiments on serum were performed using a pseudo-two-dimensional Bruker standard pulse sequence (*stddiffesgp2d*) that contained the excitation sculpting sequence for the suppression of residual HDO (700 MHz). The spectra were recorded with a spectral width of 7000 Hz, 32000 time domain data points, and two transients. The FIDs of the on and off resonance spectrum were stored and processed separately. Subtraction of the on and off resonance spectrum resulted in the STD NMR spectrum. Protein/ligand ratios of 1:260 (4.81 μM M86 antibody with 1.25 mM Gal-Gal-OMe disaccharide) and 1:200 (5.84 μM purified serum antibodies with 1.17 mM Gal-Gal-OMe disaccharide) were used.

Affinity Purification of α-Gal-specific Immunoglobulins—For purification of anti-α-Gal-specific antibodies from human serum, an α-Gal-specific affinity resin was generated. Therefore, 1 ml of Affi-Gel 10 (Bio-Rad) activated matrix was rinsed with 3 volumes of double-distilled H_2O for 20 min followed by an incubation step with 4 volumes of 100 mM HEPES buffer, pH 7.5, containing bovine thyroglobulin (70 mg/ml) for 4 h at 4 °C on a roller mixer. Remaining active esters were quenched subsequently by the addition of 100 μl of ethanolamine (1 M). Prior to first use, the affinity resin was washed with 60 volumes of PBS, pH 7.4.

To isolate α-Gal-specific antibodies, 15 ml of human serum of an α-Gal-positive donor was subjected to the aforementioned anti-Gal-specific affinity matrix. Unbound proteins were removed by washing with 100 volumes of PBS, pH 8.0, 500 mM NaCl, and α-Gal-specific antibodies were subsequently eluted into 300 μl of 1 M Tris-HCl, pH 7.5, for immediate neutralization using 700 μl of 0.1 M glycine buffer, pH 2.0. Immunoreactivity was subsequently assessed by ELISA.

Other Methods—SDS-PAGE, immunoblotting, and ELISA as well as standard procedures in molecular biology were performed according to established protocols (28).

RESULTS

Generation of α-Gal-specific Human Antibody Isotypes—To establish chimeric mouse/human antibodies, the VH and VL sequences of the α-Gal-specific antibody M86 were used as templates for gene synthesis (29). The variable regions were assembled in form of a single chain Fv, allowing prokaryotic production (supplemental Fig. 1). The antibody fragments were subsequently converted to human IgG1 and IgE isotypes by fusion with signal sequences and the particular heavy and light chain constant regions. SDS-PAGE and immunoblotting of proteins isolated from culture supernatants of stably transfected HEK-293 cells showed apparent molecular masses in the expected range of 120, 150, and 200 kDa for the homodimeric and heterotetrameric IgG and IgE antibodies, suggesting that

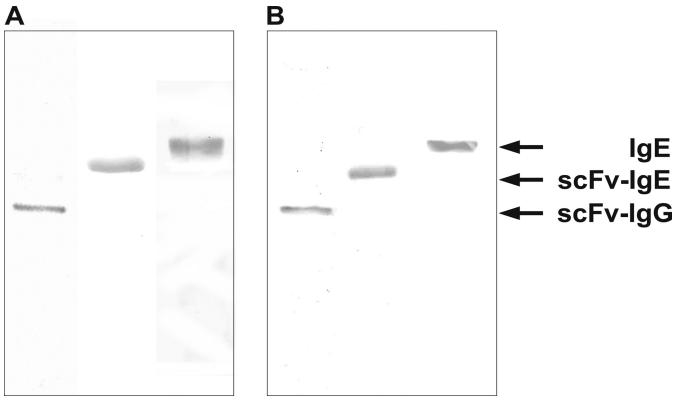

FIGURE 1. **SDS-PAGE and immunoblot analysis of IgG and IgE antibodies.** Purified proteins were assessed under non-reducing conditions by Coomassie staining (*A*) or immunoblot (*B*); the different isotypes were visualized using anti-human IgG and IgE antibodies conjugated to alkaline phosphatase.

the secreted antibodies are properly folded and glycosylated, in particular the extensively glycosylated IgE (Fig. 1).

Characterization of the Carbohydrate-specific Antibody Isotypes—Characterization of the recombinant proteins was pursued by different approaches to demonstrate both antigen and receptor binding. All antibodies detected α-Gal structures on thyroglobulin, cetuximab (not determined for IgG), and HSA conjugate in ELISA (Fig. 2*A*). Notably, the biotinylated Gal-α1,3-Gal disaccharide exhibited no interaction, a fact that might reflect the specific steric requirements of antibody binding (data not shown).

To confirm proper folding and glycosylation of the Fc domains, Ig Fc receptor extracellular domains of the ligand-binding α-chains of the human high affinity receptors FcεRI and FcγRI (CD64) fused with chicken IgG (IgY) Fc domains were used (25). Recombinant IgE as well as IgG specifically bound to their soluble Fc receptors (Fig. 2*B*). These data underline that the recombinant isotypes reflect the natural interaction with both the antigen and the cellular receptors and, therefore, should mediate comparable effects *in vivo*.

SPR analyses using immobilized IgE and cetuximab, α-Gal-HSA, and thyroglobulin as analytes resulted in k_D values in the nanomolar range (Fig. 3), which corresponds to both natural anti-Gal antibodies and carbohydrate-specific binders (30, 31). Analyses of the TNP-specific murine IgE C38–2 used below demonstrated affinities in a similar range. The HSA conjugate, however, showed a higher k_D than the other α-Gal-carrying proteins, a finding that might reflect the reduced steric accessibility as seen for the biotinylated disaccharide and a role of the missing third unit. This finding also suggests that the α-Gal valence (cetuximab < α-Gal-HSA < thyroglobulin) and the bivalent architecture of cetuximab do not significantly favor interaction.

Assessment of the Cellular Activation Potential—IgE-mediated cross-linking of the FcεRI and degranulation of RBL-SX38 cells was assessed by determination of β-hexosaminidase release (Fig. 4). Thereby, the medium affinity IgE C38-2 was used as activation control. Both anti-Gal IgE formats bound to the FcεRI and induced mediator release in an antigen-independent manner using anti-IgE antibodies to an extent comparable with the murine reference (Fig. 4*A*). Allergen-dependent cellular activation for monoclonal IgE usually is difficult to achieve, because in most cases, only one epitope per allergen is available. Here, a multivalent molecule bearing at least two independent α-Gal epitopes is needed to bridge two identical IgE paratopes. We addressed this problem using a broad panel of different α-Gal carrying proteins, including α-Gal-HSA conjugate, thyroglobulin, and cetuximab and in parallel α-Gal microspheres generated by biotinylated thyroglobulin clustered on streptavidin-coated particles (Fig. 4*B*). In contrast to the C38-2 reference that was cross-linked using a multimeric TNP-BSA-conjugate, neither the different α-Gal proteins nor α-Gal microspheres were able to induce significant mediator release (Fig. 4*B*).

These data suggest that the α-Gal IgE exhibits intrinsic potential to cross-link the FcεRI and activate effector cells, which is not translated to an antigen-dependent manner, suggesting an impact of affinity or spatial organization on α-Gal-mediated anaphylaxis.

Epitope Analysis—Variant specificities and distinct modes of binding are reported for different lectins and antibodies (32), but structural data remain scarce. Here, we aimed for a direct monitoring of the interplay of anti-Gal antibodies with the cognate antigen on a molecular level and comparability of the monoclonal IgE with polyclonal serum antibodies.

Interaction of the monoclonal chimeric IgE with the disaccharide Gal-1,3-Gal-OMe was followed by STD NMR (Fig. 5). Clear STD effects could be obtained for the carbohydrate ligand. The interaction footprint of the M86-based IgE on Gal-1,3-Gal-OMe reveals strong interaction with both galactose residues (Fig. 6*A*). Major contacts of the terminal galactose are defined by the H3 proton having the highest STD signal and, to a high extent, the H2 and H4 protons. H5, H1, and H6 also show medium STD effects. STD intensities lower than 50% most probably arise due to spin diffusion and were not included for reasons of reliability. For the adjacent galactose, major contacts are the H5 proton and H6, H3, and H4. The other protons only show minor STD effects with intensities less than our cut-off, including the methyl glycoside (Fig. 6*A*).

In parallel, polyclonal immunoglobulins were purified from serum of a donor having elevated serum IgE and IgG with specificity for α-Gal using thyroglobulin affinity chromatography. Enrichment of immunoglobulins specific for thyroglobulin was documented by ELISA (supplemental Fig. 2). Observed enrichment of anti-Gal antibodies with specificity for cetuximab suggests that the recognized moiety in the immunoglobulin preparation corresponds to those responsible for IgE-based α-Gal interaction. These antibodies then were subjected to STD NMR using the disaccharide Gal-1,3-Gal-OMe (Fig. 5).

Intriguingly, the interaction footprint of the polyclonal immunoglobulins reveals strong interaction with both galactose residues in a manner highly similar to that of the monoclonal antibody (Fig. 6, *A* and *B*). Major contacts of the terminal galactose are defined by the H2 having the highest STD signal and the H3 and H4. For the adjacent galactose, the H2 has the major contact, followed by H1 showing medium STD effects only. As above, STD intensities weaker than 50% were not included for reasons of reliability. As for the monoclonal anti-

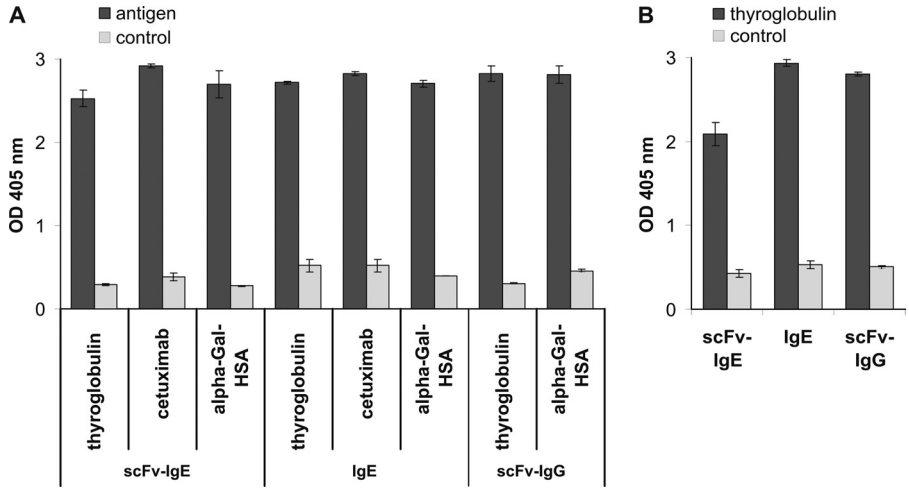

FIGURE 2. **Immunoreactivity with allergens and Fc receptor molecules.** *A*, the immunoreactivity of the recombinant human antibodies was assessed in ELISA using thyroglobulin, cetuximab, and α-Gal-HSA for the scFv-IgE and IgE and thyroglobulin and α-Gal-HSA for the scFv-IgG. Isotype-specific antibodies conjugated to alkaline phosphatase were used for detection. *B*, simultaneous binding to the allergen and Fc receptors was performed as in *A* but using the particular high affinity Fc receptors and anti-chicken IgG conjugated to alkaline phosphatase for detection. *Error bars*, S.D.

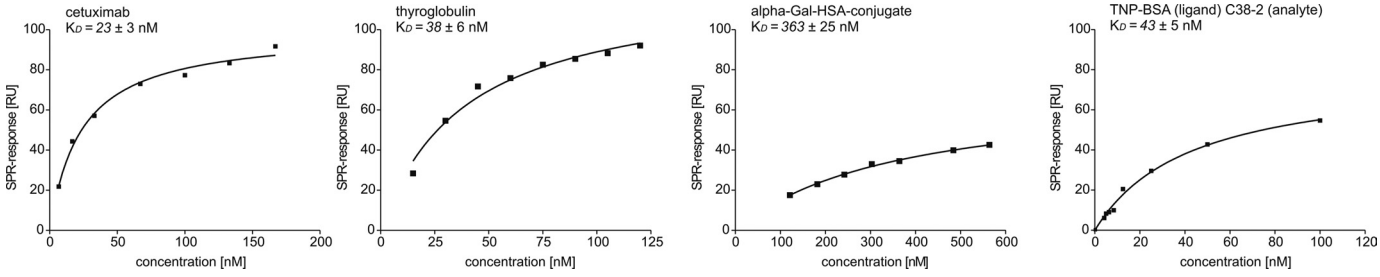

FIGURE 3. **SPR analyses of different α-Gal carriers.** The dissociation constant K_D was determined for α-Gal-HSA, thyroglobulin, and cetuximab as analytes and the scFv-IgE as immobilized ligand as well as for the TNP-specific C38-2 as analyte and TNP-BSA as immobilized ligand. The concentration-dependent curves were analyzed by the one-site binding model.

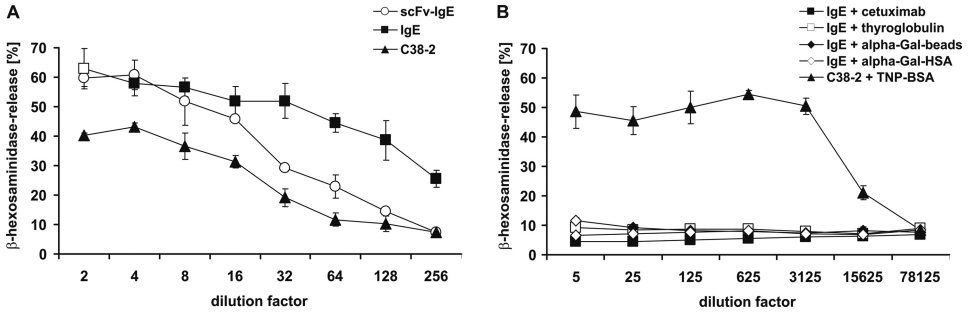

FIGURE 4. **Mediator release of humanized RBL-SX38 by α-Gal.** RBL-SX38 cells providing the human FcεRI were sensitized with the scFv-IgE, IgE, and TNP-specific mouse IgE C38-2 as control (*A*). Antigen-independent degranulation was induced by the addition of anti-human IgE and anti-murine IgE, respectively (*A*). Antigen-dependent degranulation was induced by the addition of different α-Gal-carrying proteins, including biotinylated thyroglobulin immobilized to streptavidin-coated beads, and by the addition of TNP-labeled BSA for the control (*B*). Degranulation was monitored by β-hexosaminidase activity released into culture supernatants. Data are mean ± S.D. (*error bars*) of triplicate measurements.

body, the methyl glycoside contributes to a slightly increased extent only.

These findings verify that the Gal-Gal disaccharide block is crucial and sufficient for the epitope of the monoclonal M86-based IgE as well as human polyclonal antibodies present in the circulation. The glycosidic methyl group representing the downstream residue (GlcNAc or Glc) seems to contribute weakly.

DISCUSSION

In this study, we report the construction of chimeric immunoglobulins on the basis of an α-Gal-specific antibody fragment, their application in different assay systems, and their use to define the corresponding epitope on a molecular level. Against the background of α-Gal-mediated anaphylaxis and the relevance of α-Gal as a carbohydrate epitope, our study reveals for the first time direct molecular insights into the interaction.

Generally, α1,3-Gal is considered of outstanding relevance in the context of xenotransplantation, development of biologicals, vaccine design, and reverse immunology. Consequently, specificity for α-Gal units has been assessed in different settings using a variety of reagents, including lectins, polyclonal sera, and monoclonal antibodies (32). Despite these data and recent theoretical approaches (33–35), to the best of our knowledge,

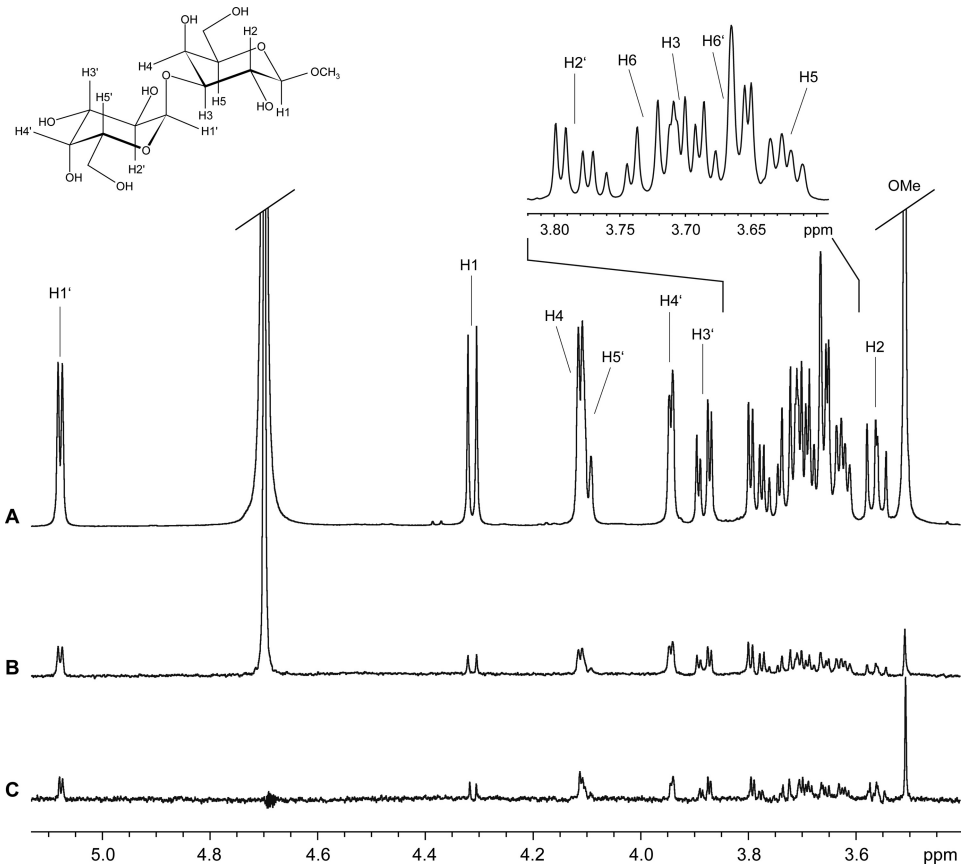

FIGURE 5. **Observation of STD signals for the α-Gal disaccharide.** Shown are the reference ^{1}H NMR spectrum (*A*) and STD NMR spectrum (*B*) of Galα1,3GalβOMe in the presence of the M86-based IgE (molecular ratio = 260:1). *C*, STD NMR spectrum of Galα1,3GalβOMe in the presence of polyclonal antibodies purified from human serum (molecular ratio = 200:1). Spectrum B has been scaled by factor 5 of its original intensity. All spectra were recorded at a temperature of 298 K and at 500 MHz with 1024 scans (*A* and *B*) and at 700 MHz with 2048 scans, respectively (*C*). STD spectra in the figure are not artifact-referenced.

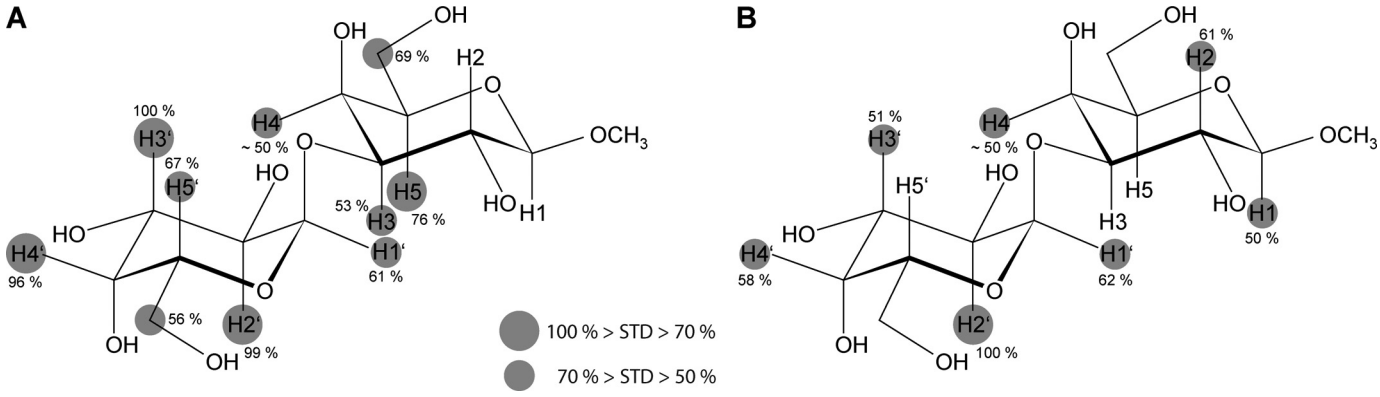

FIGURE 6. **Interaction footprint as assessed by STD NMR.** Shown are the interaction footprint of Galα1,3GalαOMe binding to M86-based IgE (*A*) and polyclonal antibodies purified from human serum (*B*). *Circles* represent the relative size of the saturation transfer and reflect the vicinity of individual protons to protons in the binding pocket of the immunoglobulin as macromolecular binding partner. The closer the ligand protons are to protons of the binding pocket, the larger is the saturation transfer. Proton H4 could not be determined with high accuracy due to resonance overlap.

no direct structural data on the important α-Gal interaction with anti-Gal antibodies are available.

In contrast to the beneficial role of α-Gal as natural barrier, its role in anaphylaxis mediated by α-Gal-specific IgE has been evolved very recently, and no IgE-based reagents have been established so far. In our study, the murine hybridoma clone M86 was chosen for conversion into human isotypes and further analyses. This antibody was established in mice after disruption of the corresponding galactosyltransferase, resembling the human system better than any other animal model (30). Human/mouse chimeric IgG and IgE produced on the basis of this antibody therefore most likely mimic the specificities observed in humans and may act as a fundament for dissection of IgE-mediated α-Gal-based anaphylaxis. The immunoreactivity of the recombinant antibodies and the functional binding to the high affinity receptors FcεRI and FcγRI generally verify their applicability in various types of immunological and allergy diagnostic backgrounds.

Although IgE generally is hypothesized as a highly affinity-matured isotype, controversy exists regarding the particular affinities of allergen-specific IgE and IgG antibodies and their physiological relevance (36). In contrast to protein-specific antibodies, however, carbohydrate-specific antibodies mostly exhibit low to medium affinities, a finding that holds true for most lectins often exhibiting affinities in the micromolar range. Although some hints exist (37), it remains unknown if IgE antibodies exhibit higher affinities in contrast to all other known carbohydrate binding structures.

The recombinant IgE generated in our study exhibited reasonable affinities as shown by SPR analyses. The real affinity, however, is difficult to assess due to the valence effects of both the bivalent antibodies and the multivalent α-Gal proteins. Anti-Gal antibodies in humans are reported to have affinities in the range of 10^{-5} to 10^{-6} M (38), which is inferior to or parallels the M86 antibody in our setting.

Here we could show that the recombinant IgE was unable to mediate basophil degranulation in the presence of multivalent α-Gal. Although the architecture of the α-Gal epitope and its availability on the surface of different carriers might affect the capability of effector cell activation, limited affinities of allergen-specific IgE can significantly decrease basophil sensitivity (39). Thus, our data suggest that class switching of preexisting IgG or IgM to IgE does not explain the anaphylactic reaction associated with α-Gal. It will be crucial and representative for all CCDs to demonstrate if anaphylaxis-mediating IgE have undergone affinity maturation processes.

On the other hand, the lack of α-Gal-dependent mediator release might also reflect the delay in anaphylactic symptoms observed for α-Gal-based allergy (12). This interpretation is favored by the fact that the murine C38-2 IgE, also of medium affinity, exhibits clear-cut cellular activation upon stimulation with a multivalent conjugate. The mechanisms underlying this retardation are the subject of speculation but now will become discernible with the antibodies generated in this study.

The structural basis of IgE B cell epitopes on allergens has been assessed by a variety of approaches (40, 41), mostly with polyclonal IgE, implying that any molecular information deduced thereof only provides indirect evidence. The most direct evidence for epitope analyses so far is the determination of crystal structures of antibody-allergen complexes. Although at first realized using murine antibodies (42–44), co-crystals revealing the nature of authentic IgE epitopes remain scarce due to the lack of human monoclonal IgE antibodies. As a result, only two structures of allergen-IgE complexes are available so far (45, 46). A peculiarity of anti-CCD antibodies is that effectual epitope is constituted by the carbohydrate itself and that it is closely related in humans and other animals. α-Gal thus represents an authentic IgE epitope, rendering this particular antibody-allergen interaction a bonanza for molecular analyses. Hence, we used a chimeric monoclonal IgE to dissect the human IgE and IgG epitopes of α-Gal by STD NMR. This technique is essentially based on the dynamics of the interaction in which the nuclear Overhauser effect is transferred to ligand residues essentially involved in binding. Differences in the free and bound state thus enable fine mapping of the interaction in a richness of detail comparable with x-ray structures only.

To our knowledge, this is the first STD NMR-based epitope mapping of an IgE epitope and one of the first examples of a human carbohydrate B cell epitope. Only two studies on carbohydrates are available that focus on the human IgG antibody 2G12 against HIV glycostructures (47) and human sera with IgG against gangliosides (48). Studies on non-human antibodies include murine IgG against Lewis-type glycans (49) and bacterial oligosaccharides (50–54).

Our application of STD NMR in this study not only provides molecular insights into the recognition of α-Gal by the immune system but also demonstrates that characterization of serum reactivities to xenobiotic epitopes can be easily addressed by STD NMR, which also is a powerful method to obtain information for individual patient sera. By deciphering the paratope-inherent information of the M86-based IgE using STD NMR, we assigned the IgE epitope primarily to the two galactose units and, to a weaker extent, to the residues downstream of the Gal-Gal unit for both the monoclonal IgE and the polyclonal immunoglobulins affinity-purified using an α-Gal carrier protein.

Although we have depicted the protons with relative STD effects of more than 50% only, most protons show limited STD effects. This phenomenon arises due to spin diffusion throughout the ligand and should be considered irrelevant without further evidence. Hence, only the protons with medium to strong effects represent carbohydrate positions important for interaction. The epitope, as suggested from the STD NMR data, is primarily comprised by the H2, H3, and H4 protons of the terminal galactose and the H3, H4, H5, and H6 protons for the adjacent galactose (H1, H2, and H4 for the human serum).

Generally, the somewhat more pronounced signals evident for the terminal galactose suggest a stronger implication in the carbohydrate-antibody interaction, a fact that is in good accordance with an end-on binding mode reported for glycan-specific binding molecules and relevance of the 1,3-linkage, which is crucial for recognition. Nevertheless, the adjacent galactose is also essentially involved in the interaction. The STD effect on the terminal OMe group is insignificant, reflecting the minor contributions of the third sugar moiety. This moiety is postulated to only modulate binding, although it is crucial for some carbohydrate binding proteins and antibodies. Human serum, however, also shows pronounced reactivity for the Gal-Gal disaccharide, indicating that the underlying principle is the recognition of the galactose dimer. It will be interesting, however, to assess the interaction of anti-Gal antibodies using a broad panel of other carbohydrates.

Of particular interest is the finding that the interaction foot print of human serum, in contrast to the monoclonal IgE, does not show significant signals for the H6 protons. With STD effects of ~45%, these protons most likely do not contribute in a significant manner. Lowering the cut-off, however, might suggest additional contributions but would weaken the overall reliability of the interaction footprint.

According to recent combined mapping and docking studies of α-Gal carbohydrates together with binding sites of monoclonal antibodies (34), the C6 positions of the carbohydrate play a prominent role by contributing to hydrophobic and van der

Waals interactions, and the O6 positions contribute to hydrogen bonding (33). Whether the weaker contributions of the H6 protons and the slight variances between monoclonal and serum-derived immunoglobulins as suggested by our STD data reflect methodological differences in *in silico* approaches or true differences in recognition remains to be elucidated.

Notably, the STD epitope of our antibodies with the terminal galactose resembles that of the 120-kDa lectin *Ricinus communis* agglutinin I with methyl-β-galactoside showing nearly identical distribution of STD effects with H3, H2, and H4 as most prominent protons (55). Additionally, this epitope has also been reported in STD NMR and crystallographic studies for the galactose binding *Viscum album* lectin VAA (56, 57). Similarly, galectin-1 as well as VAA could be shown to interact predominantly with the non-reducing terminus of digalactosides (58).

The binding mode appears roughly in accordance with that of other α-Gal-specific proteins, such as the *Marasmius oreades* (MOA) mushroom lectin, the only lectin with pronounced specificity for the α-Gal epitope. The crystal structure reveals that the carbohydrate binding site forms an shallow groove on the surface (31, 59) in which the protein exhibits contacts with the terminal and the adjacent galactose residue. Consequently, both galactose units are relatively tightly bound compared with the GlcNAc unit at the reducing end of the sugar. In contrast, the *Griffonia simplicifolia* isolectin GS I-B4 forms a deep pocket favoring the recognition of terminal galactose and thus broader specificity (60). The fact that the MOA accepts the fucosylated blood group antigen B, whereas the M86 antibody does not, is the best evidence for their different binding pocket structures.

Moreover, in a recent STD NMR-based analysis of bovine norovirus with the α-Gal epitope, the interaction map shows clear similarities to our antibody-derived map (61). This interaction, however, is completely abolished by an additional GlcNAc at the reducing end. Obviously, the recognition of the two galactose units is key for specific interaction, but the involvement of other parts of potential carbohydrate ligands and thus additional mechanisms of binding might differ significantly between different proteins.

The surprisingly similar interaction footprint of human serum containing anti-Gal IgE verified that the immune system in α1,3-galactosyltransferase knockout mice responds to xenobiotic structures in a manner comparable with humans and that the recognition mechanisms in humans are relatively uniform. This is of particular relevance because the anti-Gal IgE leading to cetuximab-based anaphylaxis might either represent independent clones with unique properties or derive from medium affinity IgM or IgG subjected to affinity maturation. In light of our finding, the first explanation might appear more convincing. On the other hand, the anti-Gal antibodies purified from serum using thyroglobulin affinity chromatography clearly show pronounced reactivity for cetuximab. Further studies of IgE derived from patients with cetuximab-based anaphylaxis, however, are needed to address this point in detail.

Moreover, the recognition of the α-Gal epitope by nature clearly contradicts the hypothesis deduced from crystal structures with proteins that IgE epitopes are preferably defined by large surface areas comprising several structural elements (45, 46). This epitope and probably all types of CCD epitopes represent classical IgG epitopes.

In summary, we have established IgE epitope-specific antibody isotypes that enable analyses of molecular interactions with the cellular immune response. Combinations of cellular and NMR-based strategies may contribute to dissect the complex network of allergic immune responses. The obtained molecular insights assist in understanding the nature of IgE B cell epitopes and the difficult interaction of antibodies with carbohydrate antigens.

Acknowledgment—We thank Thorsten Mix for technical assistance.

REFERENCES

1. Ishizaka, K., Ishizaka, T., and Hornbrook, M. M. (1966) *J. Immunol.* **97,** 840–853
2. Aalberse, R. C., Akkerdaas, J., and van Ree, R. (2001) *Allergy* **56,** 478–490
3. Aalberse, R. C., Koshte, V., and Clemens, J. G. (1981) *J. Allergy Clin. Immunol.* **68,** 356–364
4. Malandain, H. (2005) *Eur. Ann. Allergy Clin. Immunol.* **37,** 122–128
5. Fotisch, K., Altmann, F., Haustein, D., and Vieths, S. (1999) *Int. Arch. Allergy Immunol.* **120,** 30–42
6. Wicklein, D., Lindner, B., Moll, H., Kolarich, D., Altmann, F., Becker, W. M., and Petersen, A. (2004) *Biol. Chem.* **385,** 397–407
7. Jappe, U., Raulf-Heimsoth, M., Hoffmann, M., Burow, G., Hübsch-Müller, C., and Enk, A. (2006) *Allergy* **61,** 1220–1229
8. Mertens, M., Amler, S., Moerschbacher, B. M., and Brehler, R. (2010) *Clin. Exp. Allergy* **40,** 1333–1345
9. Bencúrová, M., Hemmer, W., Focke-Tejkl, M., Wilson, I. B., and Altmann, F. (2004) *Glycobiology* **14,** 457–466
10. Mari, A., Ooievaar-de Heer, P., Scala, E., Giani, M., Pirrotta, L., Zuidmeer, L., Bethell, D., and van Ree, R. (2008) *Allergy* **63,** 891–896
11. Chung, C. H., Mirakhur, B., Chan, E., Le, Q. T., Berlin, J., Morse, M., Murphy, B. A., Satinover, S. M., Hosen, J., Mauro, D., Slebos, R. J., Zhou, Q., Gold, D., Hatley, T., Hicklin, D. J., and Platts-Mills, T. A. (2008) *N. Engl. J. Med.* **358,** 1109–1117
12. Commins, S. P., Satinover, S. M., Hosen, J., Mozena, J., Borish, L., Lewis, B. D., Woodfolk, J. A., and Platts-Mills, T. A. (2009) *J. Allergy Clin. Immunol.* **123,** 426–433
13. Grönlund, H., Adédoyin, J., Commins, S. P., Platts-Mills, T. A., and van Hage, M. (2009) *J. Allergy Clin. Immunol.* **123,** 1189–1191
14. Commins, S. P., James, H. R., Kelly, L. A., Pochan, S. L., Workman, L. J., Perzanowski, M. S., Kocan, K. M., Fahy, J. V., Nganga, L. W., Ronmark, E., Cooper, P. J., and Platts-Mills, T. A. (2011) *J. Allergy Clin. Immunol.* **127,** 1286–1293.e6
15. Yu, P. B., Holzknecht, Z. E., Bruno, D., Parker, W., and Platt, J. L. (1996) *J. Immunol.* **157,** 5163–5168
16. Macher, B. A., and Galili, U. (2008) *Biochim. Biophys. Acta* **1780,** 75–88
17. Cygler, M., Rose, D. R., and Bundle, D. R. (1991) *Science* **253,** 442–445
18. van Roon, A. M., Pannu, N. S., de Vrind, J. P., van der Marel, G. A., van Boom, J. H., Hokke, C. H., Deelder, A. M., and Abrahams, J. P. (2004) *Structure* **12,** 1227–1236
19. Villeneuve, S., Souchon, H., Riottot, M. M., Mazie, J. C., Lei, P., Glaudemans, C. P., Kovác, P., Fournier, J. M., and Alzari, P. M. (2000) *Proc. Natl. Acad. Sci. U.S.A.* **97,** 8433–8438
20. Vyas, N. K., Vyas, M. N., Chervenak, M. C., Johnson, M. A., Pinto, B. M., Bundle, D. R., and Quiocho, F. A. (2002) *Biochemistry* **41,** 13575–13586
21. Nguyen, H. P., Seto, N. O., MacKenzie, C. R., Brade, L., Kosma, P., Brade, H., and Evans, S. V. (2003) *Nat. Struct. Biol.* **10,** 1019–1025
22. Meyer, B., and Peters, T. (2003) *Angew Chem. Int. Ed. Engl.* **42,** 864–890
23. Galili, U., LaTemple, D. C., and Radic, M. Z. (1998) *Transplantation* **65,** 1129–1132
24. Braren, I., Blank, S., Seismann, H., Deckers, S., Ollert, M., Grunwald, T., and Spillner, E. (2007) *Clin. Chem.* **53,** 837–844
25. Braren, I., Greunke, K., Pilette, C., Mempel, M., Grunwald, T., Bredehorst,

R., Ring, J., Spillner, E., and Ollert, M. (2011) *Anal. Biochem.* **412,** 134–140
26. Greunke, K., Spillner, E., Braren, I., Seismann, H., Kainz, S., Hahn, U., Grunwald, T., and Bredehorst, R. (2006) *J. Biotechnol.* **124,** 446–456
27. Gehlhar, K., Peters, M., Brockmann, K., van Schijndel, H., and Bufe, A. (2005) *Int. Arch. Allergy Immunol.* **136,** 311–319
28. Ausubel, F. M., Brent, R., Kingston, R. E., Moore, D. D., Seidman, J. G., Smith, J. A., and Struhl, K. (eds) (1994) *Current Protocols in Molecular Biology*, Greene Publishing Associates and Wiley-Interscience, New York
29. Steinberger, P., Kraft, D., and Valenta, R. (1996) *J. Biol. Chem.* **271,** 10967–10972
30. Chiang, T. R., Fanget, L., Gregory, R., Tang, Y., Ardiet, D. L., Gao, L., Meschter, C., Kozikowski, A. P., Buelow, R., and Vuist, W. M. (2000) *Transplantation* **69,** 2593–2600
31. Grahn, E., Askarieh, G., Holmner, A., Tateno, H., Winter, H. C., Goldstein, I. J., and Krengel, U. (2007) *J. Mol. Biol.* **369,** 710–721
32. Diswall, M., Gustafsson, A., Holgersson, J., Sandrin, M. S., and Breimer, M. E. (2011) *Xenotransplantation* **18,** 28–39
33. Agostino, M., Sandrin, M. S., Thompson, P. E., Yuriev, E., and Ramsland, P. A. (2010) *Glycobiology* **20,** 724–735
34. Agostino, M., Sandrin, M. S., Thompson, P. E., Yuriev, E., and Ramsland, P. A. (2009) *Mol. Immunol.* **47,** 233–246
35. Milland, J., Yuriev, E., Xing, P. X., McKenzie, I. F., Ramsland, P. A., and Sandrin, M. S. (2007) *Immunol. Cell Biol.* **85,** 623–632
36. Fromberg, J. (2006) *Allergy* **61,** 1234
37. Jin, C., Hantusch, B., Hemmer, W., Stadlmann, J., and Altmann, F. (2008) *J. Allergy Clin. Immunol.* **121,** 185–190.e2
38. McKenzie, I. F., Patton, K., Smit, J. A., Mouhtouris, E., Xing, P., Myburgh, J. A., and Sandrin, M. S. (1999) *Transplantation* **67,** 864–870
39. Christensen, L. H., Holm, J., Lund, G., Riise, E., and Lund, K. (2008) *J. Allergy Clin. Immunol.* **122,** 298–304
40. Gehlhar, K., Rajashankar, K. R., Hofmann, E., Betzel, C., Weber, W., Werner, S., and Bufe, A. (2006) *Int. Arch. Allergy Immunol.* **140,** 285–294
41. Hantusch, B., Krieger, S., Untersmayr, E., Schöll, I., Knittelfelder, R., Flicker, S., Spitzauer, S., Valenta, R., Boltz-Nitulescu, G., Scheiner, O., and Jensen-Jarolim, E. (2004) *J. Allergy Clin. Immunol.* **114,** 1294–1300
42. Li, M., Gustchina, A., Alexandratos, J., Wlodawer, A., Wünschmann, S., Kepley, C. L., Chapman, M. D., and Pomés, A. (2008) *J. Biol. Chem.* **283,** 22806–22814
43. Padavattan, S., Schirmer, T., Schmidt, M., Akdis, C., Valenta, R., Mittermann, I., Soldatova, L., Slater, J., Mueller, U., and Markovic-Housley, Z. (2007) *J. Mol. Biol.* **368,** 742–752
44. Mirza, O., Henriksen, A., Ipsen, H., Larsen, J. N., Wissenbach, M., Spangfort, M. D., and Gajhede, M. (2000) *J. Immunol.* **165,** 331–338
45. Niemi, M., Jylhä, S., Laukkanen, M. L., Söderlund, H., Mäkinen-Kiljunen, S., Kallio, J. M., Hakulinen, N., Haahtela, T., Takkinen, K., and Rouvinen, J. (2007) *Structure* **15,** 1413–1421
46. Padavattan, S., Flicker, S., Schirmer, T., Madritsch, C., Randow, S., Reese, G., Vieths, S., Lupinek, C., Ebner, C., Valenta, R., and Markovic-Housley, Z. (2009) *J. Immunol.* **182,** 2141–2151
47. Enríquez-Navas, P. M., Marradi, M., Padro, D., Angulo, J., and Penadés, S. (2011) *Chemistry* **17,** 1547–1560
48. Houliston, R. S., Jacobs, B. C., Tio-Gillen, A. P., Verschuuren, J. J., Khieu, N. H., Gilbert, M., and Jarrell, H. C. (2009) *Biochemistry* **48,** 220–222
49. Herfurth, L., Ernst, B., Wagner, B., Ricklin, D., Strasser, D. S., Magnani, J. L., Benie, A. J., and Peters, T. (2005) *J. Med. Chem.* **48,** 6879–6886
50. Maaheimo, H., Kosma, P., Brade, L., Brade, H., and Peters, T. (2000) *Biochemistry* **39,** 12778–12788
51. Oberli, M. A., Tamborrini, M., Tsai, Y. H., Werz, D. B., Horlacher, T., Adibekian, A., Gauss, D., Möller, H. M., Pluschke, G., and Seeberger, P. H. (2010) *J. Am. Chem. Soc.* **132,** 10239–10241
52. Clément, M. J., Fortuné, A., Phalipon, A., Marcel-Peyre, V., Simenel, C., Imberty, A., Delepierre, M., and Mulard, L. A. (2006) *J. Biol. Chem.* **281,** 2317–2332
53. Niedziela, T., Letowska, I., Lukasiewicz, J., Kaszowska, M., Czarnecka, A., Kenne, L., and Lugowski, C. (2005) *Infect. Immun.* **73,** 7381–7389
54. Kooistra, O., Herfurth, L., Lüneberg, E., Frosch, M., Peters, T., and Zähringer, U. (2002) *Eur. J. Biochem.* **269,** 573–582
55. Mayer, M., and Meyer, B. (2001) *J. Am. Chem. Soc.* **123,** 6108–6117
56. Mikeska, R., Wacker, R., Arni, R., Singh, T. P., Mikhailov, A., Gabdoulkhakov, A., Voelter, W., and Betzel, C. (2005) *Acta Crystallogr. Sect. F Struct. Biol. Cryst. Commun.* **61,** 17–25
57. Martín-Santamaría, S., André, S., Buzamet, E., Caraballo, R., Fernández-Cureses, G., Morando, M., Ribeiro, J. P., Ramírez-Gualito, K., de Pascual-Teresa, B., Cañada, F. J., Menéndez, M., Ramström, O., Jiménez-Barbero, J., Solís, D., and Gabius, H. J. (2011) *Org. Biomol. Chem.* **9,** 5445–5455
58. Miller, M. C., Ribeiro, J. P., Roldos, V., Martin-Santamaria, S., Canada, F. J., Nesmelova, I., Andre, S., Pang, M., Klyosov, A., Baum, L. G., Jimenez-Barbero, J., Gabius, H. J., and Mayo, K. H. (2011) *Glycobiology*, in press
59. Grahn, E. M., Winter, H. C., Tateno, H., Goldstein, I. J., and Krengel, U. (2009) *J. Mol. Biol.* **390,** 457–466
60. Tempel, W., Tschampel, S., and Woods, R. J. (2002) *J. Biol. Chem.* **277,** 6615–6621
61. Zakhour, M., Ruvoën-Clouet, N., Charpilienne, A., Langpap, B., Poncet, D., Peters, T., Bovin, N., and Le Pendu, J. (2009) *PLoS Pathog.* **5,** e1000504